ELSEVIER

Computational Materials Science 24 (2002) 421–429

COMPUTATIONAL MATERIALS SCIENCE

www.elsevier.com/locate/commatsci

Pressure-transmitting boundary conditions for molecular-dynamics simulations

Carsten Schäfer [a], Herbert M. Urbassek [a,*], Leonid V. Zhigilei [b], Barbara J. Garrison [c]

[a] *Fachbereich Physik, Universität Kaiserslautern, Erwin-Schrödinger-Straße, D-67663 Kaiserslautern, Germany*
[b] *Department of Materials Science and Engineering, University of Virginia, Charlottesville, VA 22903, USA*
[c] *Department of Chemistry, 152 Davey Laboratory, Pennsylvania State University, University Park, PA 16802, USA*

Received 10 October 2001; accepted 20 November 2001

Abstract

A scheme for establishing boundary conditions in molecular-dynamics simulations that prevent pressure wave reflection out of the simulation volume is formulated. The algorithm is easily implemented for a one-dimensional geometry. Its efficiency is tested for compressive waves in Cu. © 2002 Elsevier Science B.V. All rights reserved.

PACS: 02.70.Ns

1. Introduction

Molecular-dynamics calculations are generally used to simulate macroscopic systems containing a large number (in the order of Avogadro's number, 10^{23}) of atoms. By necessity, the simulation concentrates on a small part of the system, on the order of several hundreds [1] to a maximum [2] of nowadays 5×10^9 atoms. This reduction in system size is possible, if convenient boundary conditions are applied to the simulation volume; these boundary conditions are chosen to mimic the response of the surrounding material to the processes occurring in the simulation volume itself.

The boundary conditions applicable to simulations in thermodynamic equilibrium (static response) have been well studied in the past [3–6]. However, nowadays, often non-equilibrium processes are to be simulated. Then the formulation of the appropriate boundary conditions poses a larger challenge, as they need to incorporate the dynamic response of the surroundings to the processes occurring in the simulation volume. Thus, for example, if heat is produced in the simulation volume, the boundaries have to dispense of it in a realistic way, mimicking the natural heat conduction of the solid. This can be achieved using so-called energy-dissipating boundary conditions [7,8]. This problem arises, e.g., when energetic processes, such as ion or laser irradiation of a solid

* Corresponding author.
E-mail address: urbassek@rhrk.uni-kl.de (H.M. Urbassek).
URL: http://www.physik.uni-kl.de/urbassek.

0927-0256/02/$ - see front matter © 2002 Elsevier Science B.V. All rights reserved.
PII: S0927-0256(01)00263-4

surface, are simulated [7,9]. Analogously, stress produced in the simulation volume has to be relaxed at the boundaries in a way compatible with the elastic properties of the solid. Again, this is quite a commonly encountered phenomenon in irradiation or impact simulations [10,11].

The latter class of boundary conditions is more difficult to formulate. In fact, a number of schemes have been published recently to solve this problem that are based on a generalized Langevin approach [12–14], in which the reaction of the surrounding is incorporated into the dynamical equations of the simulation volume via (delayed) forces [15,16]. It turns out, however, that the calculation of these boundary conditions is rather time consuming. For this reason, we propose in this paper a simple phenomenological scheme to handle pressure relaxation and pressure wave transmission, which is easy to implement and adds virtually no extra computational costs to the simulation. This scheme was introduced in Ref. [17], and used repeatedly for applications in laser ablation of solids [11,18,19]. We shall validate the scheme for a metallic system by investigating its ability to transmit pressure waves.

2. Formulation of boundary conditions

2.1. Passage of a pressure wave through matter

In order to set the stage, we remind the reader of the basic properties of a pressure wave in a solid. Fig. 1 exemplifies the conditions in a material through which a pressure wave passes. The figure was taken from a molecular-dynamics simulation of Cu; the wave was started by applying a sudden force perpendicular to the surface (for details see Section 3 below). The quantities discussed below denote local averages; they were determined in the simulation as averages over a distance of $r_c = 6.2$ Å, the cutoff radius of our potential.

The pressure wave runs with a velocity of 55 Å/ps, which is 25% above the speed of sound, which is $c_0 = 44$ Å/ps for a longitudinal wave in Cu in the [1 0 0] direction; it is hence a (moderately) weak pressure wave [20]. In the wave itself, the density n is increased by around 10% above the nominal crystal density $n_0 = 0.085$ Å^{-3}. In the region of enhanced density—between 27 and 35 Å, roughly—the atom velocity u is non-vanishing; its values, however, are small compared to c_0. The pressure p, however, starts to become already strong in the leading part of the wave, before atoms have reached sizable velocities. This is in contrast to a well-known relationship [21], which has pressure to be proportional to the atom velocity

$$p = -mn_0c_0u = -Zu, \tag{1}$$

where m is the atom mass, and $Z = mn_0c_0$ is called the impedance of the system; in our case, $Z = 3.96$ GPa/(Åps) $= 24.7$ meVps/Å^4. Inspection of Fig. 1b and c shows that this simple proportionality does not hold on the microscopic (atomistic) scale. It is the purpose of the following section to show that a closely related proportionality does indeed hold for a well-defined part of the forces acting on an atom, viz. Eq. (4) below.

2.2. Boundary forces

As soon as such a pressure wave reaches the boundary of the simulation volume, it will be reflected. This happens for both types of boundary conditions commonly applied, namely free and fixed boundaries. In order to prevent reflection, one has to mimic the action of the surrounding medium on the atoms close to the boundary. We do this in the following way: we define as boundary zone the part of the simulation volume adjacent to the boundary (cf. Fig. 2); its width Δz must be (slightly) larger than r_c. Atoms in the rest of the simulation volume (the MD zone) obey the original MD equations of motion with forces stemming from the neighboring atoms. Thus in Fig. 2, atom i experiences a force F stemming from all atoms j surrounding it. Let us write F as

$$F = F_{\text{top}} + F_{\text{bottom}}, \tag{2}$$

where F_{top} is the force originating from all atoms above i (i.e., away from the boundary), and F_{bottom} is the force originating from all atoms below it (i.e., closer to the boundary). Here and in the following we shall be interested only in the force components

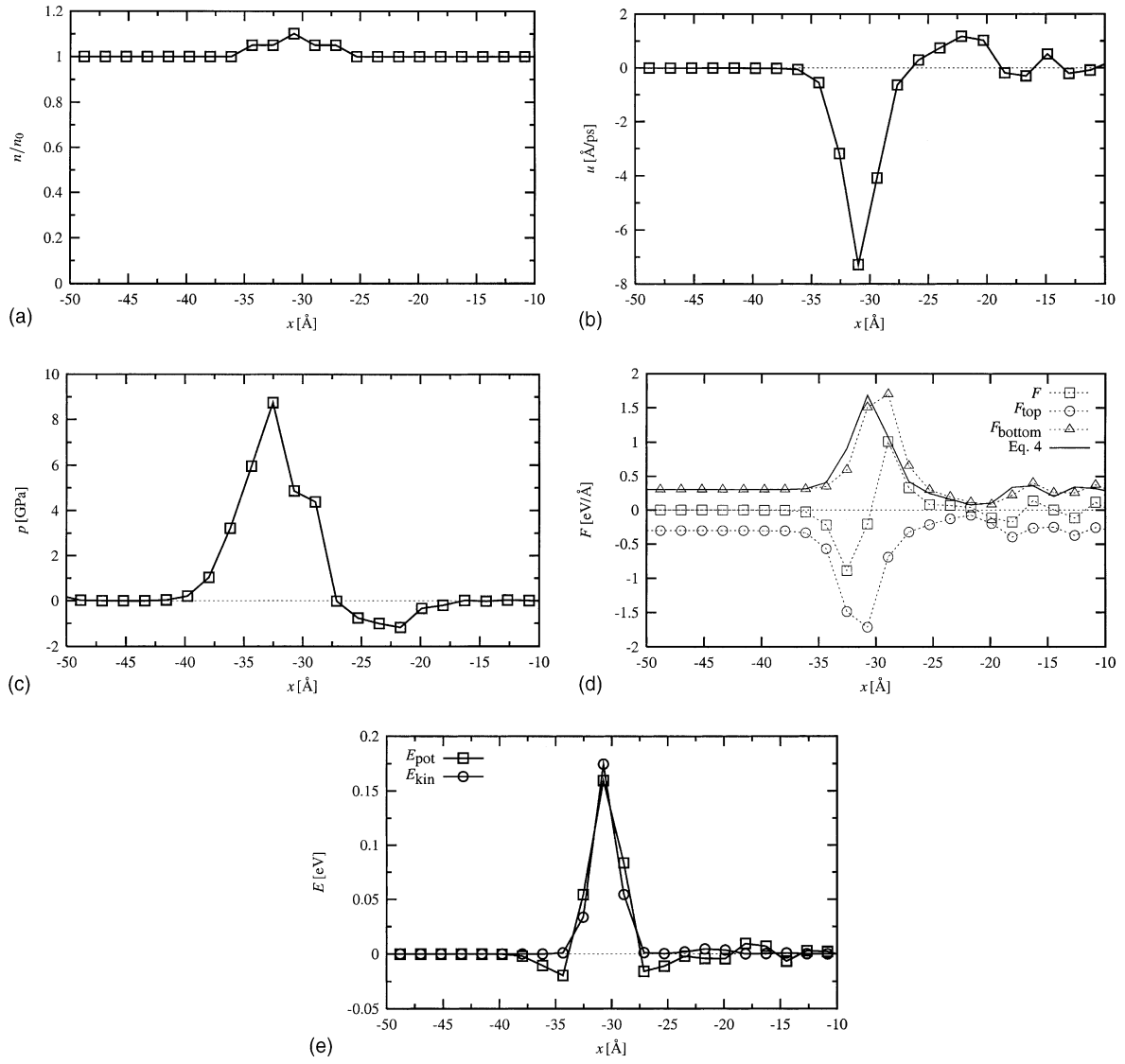

Fig. 1. Molecular-dynamics results of a pressure wave travelling through a Cu crystallite in [1 0 0] direction. The wave was excited by applying a force $K = 7.5$ eV/Å for 11 fs on each surface atom in the direction perpendicular to the surface. The data were taken at 0.6 ps after pulse excitation. (a) Density n, (b) atom velocity u, (c) pressure p, (d) force F split into top and bottom part, F_{top} and F_{bottom}, respectively, according to Eq. (2), cf. Fig. 2, thick line: Eq. (4), (e) potential and kinetic energy, E_{pot} and E_{kin}, respectively.

perpendicular to the boundary; hence we can abstain from using vector notation.

Fig. 1d shows F and its two components F_{top} and F_{bottom} in a pressure pulse. We observe that F_{top} and F_{bottom} have a simple unimodal shape, while the total force F shows the more complex structure typical of a pressure pulse, consisting of an accelerating and a decelerating part.

While using interatomic interaction to determine both F_{top} and F_{bottom} in the molecular-dynamics

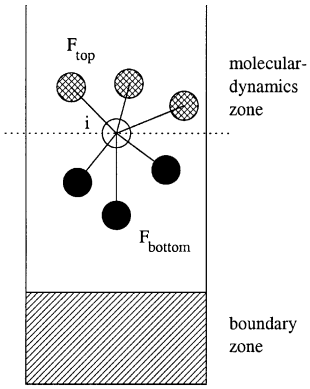

Fig. 2. Schematics of the simulation volume, partitioned into a boundary zone, and the MD zone proper. Forces on an atom i are shown. Forces are split into F_{top} (arising from atoms further away from the boundary) and F_{bottom} (arising from atoms closer to the boundary).

zone, in the boundary zone we model F_{bottom} by a simple expression F_{bc} such that atoms in the boundary zone experience a total force

$$F = F_{\text{top}} + F_{\text{bc}}, \tag{3}$$

in analogy to Eq. (2). F_{top} is calculated from the interatomic potentials in the same way as in the MD zone. The boundary force, F_{bc}, is directed perpendicular to the boundary. Its magnitude is determined as

$$F_{\text{bc}} = F_0 - \alpha u. \tag{4}$$

Here, F_0 is a static contribution, which is present even if atoms do not move. It is needed to keep the crystal in equilibrium, to counter the force of the top atoms and to eliminate the surface tension forces acting on the atoms in the boundary region. The second part of the force, Eq. (4) is proportional to the velocity u of the atoms in the boundary. For the purposes of this paper—short pulses and low ambient temperatures—it is appropriate to take u as the velocity of the individual boundary atom. More generally, this procedure would induce an artificial cooling of the boundary, and u should be taken as the average velocity (center-of-mass velocity) of all atoms in the boundary [17]. According to Eq. (1), we choose the proportionality constant α as

$$\alpha = ZA = mn_0c_0A, \tag{5}$$

where A is the cross-sectional area of an atom. Thus, Eq. (4) makes sure that the atoms in the boundary zone are subject to the pressure, Eq. (1), that they need to feel under the passage of a pressure pulse. By prescribing the correct impedance to the boundary we prevent acoustic waves from reflecting. We shall hence refer to α as the impedance coefficient in this paper. Note that $\zeta = \alpha/m$ may be interpreted as a friction coefficient in Eq. (4). Since A is of the order of $n_0^{-2/3}$, ζ is proportional to the Debye frequency $\omega_{\text{D}} = \sqrt[3]{6\pi^2 n_0}\cdot\bar{c}$, where $\bar{c}$ is an appropriately averaged speed of sound. A friction of $\zeta_{\text{AD}} = \pi\omega_{\text{D}}/6$ was indeed derived by Adelman and Doll [12] in their generalized Langevin approach by using a Brownian approximation.

We emphasize that the boundary zone must be determined dynamically during the simulation, to keep it a width Δz above the bottommost atom layer; its absolute position and even the identity of its atoms can change during the simulation.

2.3. Determination of parameters

In the following, we shall discuss the determination of the parameters necessary to implement the boundary conditions. We shall do this specifically for a many-body potential as it is adequate for a metal, such as the EAM potential [22]. The implementation for two-body potentials can be viewed as a special case of this more general type of potentials by setting the many-body embedding function equal to zero. We shall establish the parameters here for the many-body potential defined in Ref. [23].

For many-body forces, the partitioning of the (well-defined) total force into F_{top} and F_{bottom} needs an explication. We proceed as follows: let us write the total potential energy of the crystal as

$$E_{\text{tot}} = \sum_{i<j} \Phi(r_{ij}) + \sum_i G(\rho_i), \tag{6}$$

with

$$\rho_i = \sum_{j\neq i} g(r_{ij}). \tag{7}$$

Here Φ is a pair potential, G the embedding function, and g the atomic contribution to ρ_i, the

so-called electron density. Then the total force on atom i is

$$\mathbf{F}_i = \sum_{j \neq i} \mathbf{F}_{ij}, \tag{8}$$

where

$$\mathbf{F}_{ij} = -\{\Phi'(r_{ij}) + g'(r_{ij})[G'(\rho_i) + G'(\rho_j)]\}\mathbf{e}_{ij}. \tag{9}$$

Here the dash denotes differentiation with respect to the argument and $\mathbf{e}_{ij}$ is the unit vector pointing from atom j to atom i. $\mathbf{F}_{ij}$ may be interpreted as the force contributed by atom j to the total force on atom i; this makes the partitioning of $\mathbf{F}_i$ into F_{top} and F_{bottom} by the position of atom j with respect to atom i obvious.

We note that these formulae allow us to calculate F_0, and hence the static part of the boundary force, analytically. Alternatively, F_0 can be conveniently determined from a static simulation of the crystal in equilibrium (pressure $p = 0$). Both procedures yield $F_0 = 0.302$ eV/Å.

The dynamical part of the boundary force is governed by the parameter α. Using Eq. (5), it could be determined from the impedance of the crystal and the atomic cross-section, which (for the (1 0 0) surface) may be set equal to $A = a^2/2 = 6.53$ Å^2. This gives a value of $\alpha_{\text{theor}} = 0.162$ eVps/Å^2, corresponding to a friction coefficient $\zeta = 2c_0/a = 24.4$/ps.

As an alternative procedure, we may determine α by performing a dynamical simulation of a pressure wave travelling through a crystal. The dependence of F_{bottom} on the velocity u in a region far away from all boundaries can thus be determined. The result of such a simulation is shown in Fig. 3a. It is seen that F_{bottom} correlates quite well with the individual velocity of each atom. A linear fit gives $\alpha_{\text{simul}} = 0.193$ eVps/Å^2, in quite good agreement with the estimate α_{theor} given above. We plotted F_{bc} according to Eq. (4) with parameters as discussed above also in Fig. 1d. Good agreement with the simulated values of F_{bottom} is observed. Note, however, that in the leading part of the pulse, F_{bc} overestimates F_{bottom}, while it underestimates it in the trailing part.

We note that we performed the same fit for a soft material, condensed Ar. The results, obtained for a Lennard–Jones pair potential [24], are shown in Fig. 3b. Here for negative velocities, a bi-valued result is obtained. This sort of hysteresis behavior is analogous—but more pronounced—to the behavior found for Cu and discussed above: in the leading (trailing) part of the wave smaller (larger) forces than predicted by Eq. (4) occur. A linear fit is then useful only as an average or for one part of the hysteresis loop.

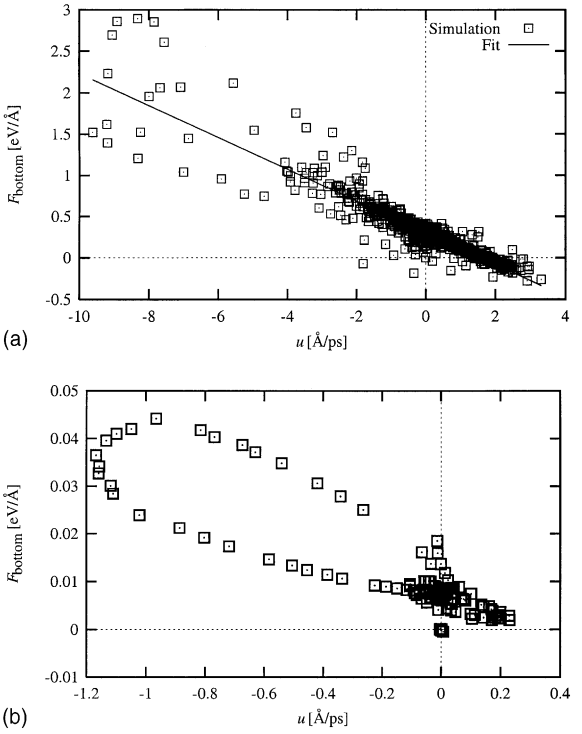

Fig. 3. Dependence of the force F_{bottom} acting on individual atoms vs their velocity u. Simulation data for a pressure wave travelling in (a) Cu and (b) Ar. Line: fit to Eq. (4).

3. Validation

We shall use in this paper Cu as a model system to exemplify and test our scheme. The molecular-dynamics simulation employs the many-body potential defined in Ref. [23]; this is of the so-called embedded-atom [22] or tight-binding [25] form. The simulation employs a Cu crystallite at 0 K with a (1 0 0) surface and a cross-sectional area of $(6a)^2$, where $a = 3.615$ Å is the Cu lattice constant.

While the surface is left free, lateral periodic boundary conditions are applied at all four sides. At the bottom of the simulation volume, we shall employ the pressure-transmitting boundary conditions, which are the subject of this paper.

A convenient way to test our scheme is to measure to which degree the boundary conditions are able to prevent pressure waves from reflection. To this end we prepare a pressure wave by applying a force K for a short period of time (here: $\Delta t = 11$ fs) on each surface atom in the direction perpendicular to the surface. Fig. 1 showed the form of the resulting pressure wave in the material for a value of $K = 7.5$ eV/Å.

In order to quantify wave reflection, we introduce the reflection coefficient

$$R = E_{\mathrm{refl}}/E_{\mathrm{in}}, \tag{10}$$

where E_{in} is the (constant) kinetic energy in the wave before reaching the boundary and E_{refl} is the kinetic energy in the crystal after wave reflection. We measured E_{refl} some time after wave reflection, when it had become constant.

Let us first test whether the parameters F_0 and α appearing in the boundary force, Eq. (4), were optimal in preventing wave reflection. For this test, we fixed the wave strength to $K = 7.5$ eV/Å, and let the wave interact with a boundary with varying values of F_0 and α in the boundary force. Fig. 4 displays the variation of the reflection coefficient with F_0 and α. The optimum reflectivity R_{opt} reaches a value of only 3.15%, which is sufficiently small for many applications. Note that our pressure wave is very sharp; as was shown in Ref. [15], it can be assumed that the reflection of waves with less steep boundaries will be even more reduced than the sharp wave studied by us.

R_{opt} occurs for the value of F_0 determined in Section 2.3; however, the corresponding value of $\alpha = 0.21$ eVps/Å^2 is somewhat larger than that found in Section 2.3 from Fig. 3, $\alpha_{\mathrm{simul}} = 0.193$ eVps/Å^2. The reason for this increase in the optimum value of α may lie in the strength of our pressure pulse. We therefore performed another determination of F_0 and α for a really weak wave, excited with a force $K = 0.75$ eV/Å. Then the parameter dependence is even more pronounced. Furthermore, the optimum value of α has decreased from 0.21 to a value of 0.19 eVps/Å^2, i.e., the value determined from Fig. 3 in Section 2.3. This is due to the fact that for the weak wave, the wave speed is identical to the speed of sound c_0. We note that also the scatter in the F_{bottom} vs u correlation is reduced (not shown).

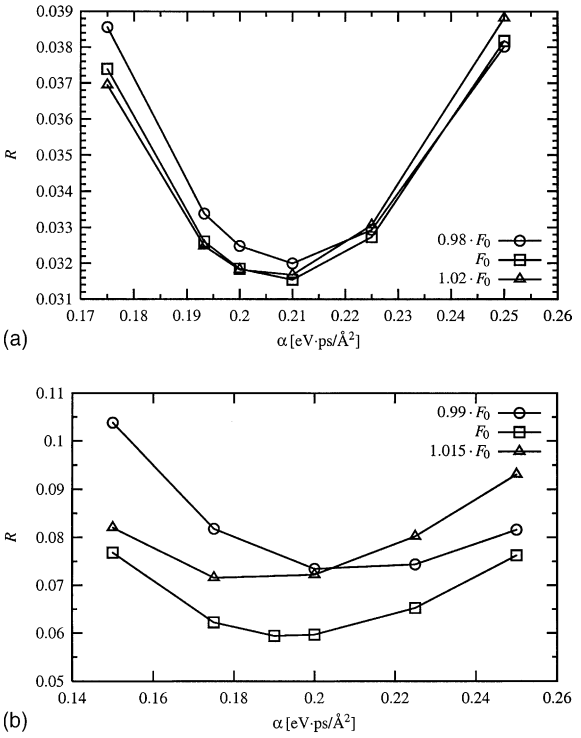

Fig. 4. Reflection coefficient R of a weak pressure wave—excited by a force (a) 7.5 eV/Å and (b) 0.75 eV/Å—vs the boundary impedance coefficient α. The curve parameter is the constant contribution F_0 to the boundary force.

Note that R is not very sensitive to changes of the impedance coefficient α in the order of 10%; this is helpful, since the determination of α occurred either by the determination of crystal parameters like c_0, n_0, A, which may not be known to an accuracy better than 10 % (note that in particular the wave speed may increase with wave strength!); or by a fitting procedure as displayed in Fig. 3, which again is subject to some error. On the other hand, the dependence of R on F_0 is quite pronounced, and changes of F_0 by a few % change R distinctly. As outlined above, however, F_0 can be safely determined with high accuracy analytically or by a static simulation.

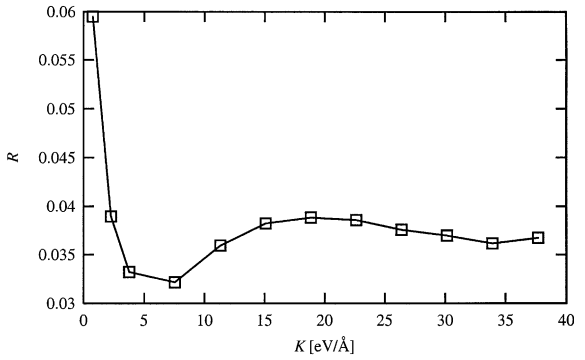

Fig. 5. Reflection coefficient R vs strength K exciting the pressure wave. Parameters F_0 and α as determined in Section 2.3.

Fig. 5 shows how R varies with the strength of the pressure wave. Here the optimum value of $\alpha_{\text{simul}} = 0.193$ eVps/Å^2 as determined in Section 2.3 has been kept. In particular that we did not optimize α for each value of the force K. Note that R is between 3% and 4% for a wide range of wave strengths, and only increases towards very weak waves. The reason hereto lies in the fact that these quite weak waves become very delocalized during the simulation, and look more like an acoustic wave rather than a pressure pulse. These longer wave trains transmit less efficiently through the boundary zone than a well localized pulse. Thus, the boundary impedance seems to work fine even for stronger waves, where the wave speed is definitely larger than c_0.

4. Summary

- We formulated a conceptually simple and easy-to-implement method which allows to minimize pressure wave reflection at the boundary of a molecular-dynamics simulation volume.
- The method is easily adapted to a variety of materials, including those with many-body interaction forces.
- Two parameters need to be determined for implementing the boundary force. We discuss several ways to determine these, and measure the sensitivity of the method to the accuracy of choosing the parameters.
- We find pressure wave reflection to be suppressed by our method to a level of 3–4% which is adequate for many applications.

Acknowledgements

The authors are grateful to M. Moseler and G. Williams for discussions. They thank the computer center RHRK, University of Kaiserslautern, for making available computer time for this study.

Appendix A. Microscopic processes during pulse passage

In this appendix, we shall study how the kinetic, potential and total energies summed over all atoms in the crystal change when a pressure pulse impinges on the boundary zone. Throughout this appendix, we shall study a pulse excited with a force of 7.5 eV/Å. Let us first study (Fig. 1e) the spatially resolved energy content of the pressure pulse displayed in Fig. 1. E_{pot} has been set to zero for a crystal in equilibrium. We observe again the rather pronounced sharp front, followed by a rather long, but considerably weaker tail. Note that the front part of the pulse has negative potential energy. This is a feature common to all realistic potentials stretching out further than the nearest-neighbor distance: atoms in front of the pulse feel approaching atoms, and hence the bonding (attraction) increases. Only when nearest-neighbor atoms come close, does repulsion set in, and the potential energy becomes positive.

As a reference case, in Fig. 6, we display the temporal changes of the kinetic and potential energies in a crystal of 30 ML length when the pressure pulse impinges on a free surface. The pressure pulse needs about 0.1 ps to equilibrate potential and kinetic energy. Note that $E_{\text{kin}} > E_{\text{pot}}$, since the pulse is strong enough that the crystal forces become anharmonic. At 1 ps, the pulse is reflected: at the free surface the crystal almost completely relaxes ($E_{\text{pot}} = 0$) while all energy is converted to kinetic energy. The pulse shape changes upon reflection; hence the oscillations visible after reflection.

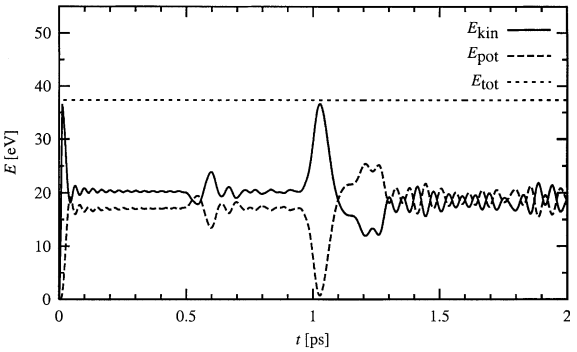

Fig. 6. Molecular-dynamics results of a pressure wave travelling through a 30 ML Cu crystallite in [1 0 0] direction, cf. Fig. 1. Time dependence of potential, kinetic and total energy (E_{pot}, E_{kin}, and E_{tot}, respectively) summed over all atoms in the crystal. Free boundary conditions.

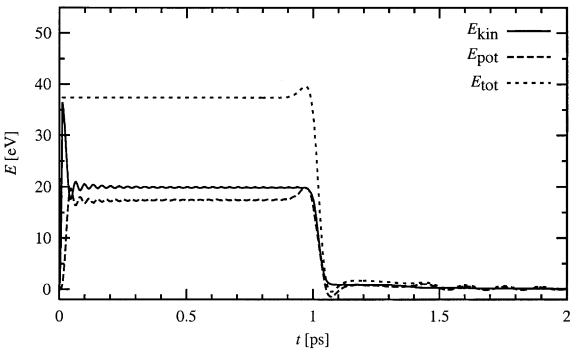

Fig. 7. Molecular-dynamics results of a pressure wave travelling through a 60 ML Cu crystallite in [1 0 0] direction, cf. Fig. 1. Time dependence of potential, kinetic and total energy (E_{pot}, E_{kin}, and E_{tot}, respectively) summed over the top 30 ML in the crystal.

Fig. 7 shows pulse transmission through an 'ideal boundary': this was realized by using a large crystal (60 ML) and measuring the energies only in the first 30 ML. Upon passage the kinetic energy drops very sharply (within 50 fs) to about 5% of its initial value. The later decrease to 0% is quite slow, and takes more than 1 ps; this is due to the pulse tail shown in Fig. 1e. The potential energy shows somewhat more structure: immediately before pulse passage it increases; this occurs when the front part of the pulse possessing negative potential energy (Fig. 1e) has passed the ideal boundary. Immediately after passage, it decreases (even

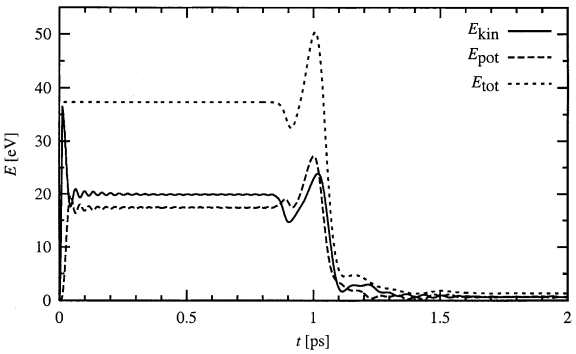

Fig. 8. Same as Fig. 6, but for pressure-transmitting boundary conditions.

below 0!); this is due to the oscillatory nature of the pulse visible in Fig. 1e. Note that the total energy within the first 30 ML slightly increases immediately before the pulse leaves the zone. This happens when the attractive part of the pulse (cf. Fig. 1e) just has passed into the lower 30 ML.

Finally, Fig. 8 shows what happens when the pulse impinges on the boundary zone presented in this paper. The strong decrease of the energy at 1.1 ps proves that this boundary zone essentially acts like the ideal boundary. However, several differences are seen in detail. When the pulse enters the boundary zone, at first atoms are decelerated due to the action of the boundary force, Eq. (4). Then, at $t \cong 1$ ps, atoms are accelerated, in close analogy to what happens at a free boundary, Fig. 6. However, while there the crystal relaxed almost completely to $E_{pot} = 0$, E_{pot} increases in the boundary zone, since atom motion is hindered, and hence repulsive forces dominate. Also after pulse passage, $t > 1$ ps, the energies show a temporal dependence different from that of the ideal boundary, Fig. 7; and in particular not all energy leaves the crystal.

References

[1] B.J. Alder, T.E. Wainwright, J. Chem. Phys. 27 (1957) 1208.
[2] J. Lau, MRS Bull. 25 (9) (2000) 5.
[3] M.P. Allen, D.J. Tildesley (Eds.), Computer simulation of liquids, Clarendon, Oxford, 1987.

[4] J.M. Haile, Molecular dynamics simulation: elementary methods, Wiley, New York, 1992.
[5] D.C. Rapaport, The Art of Molecular Dynamics Simulation, Cambridge University Press, Cambridge, 1995.
[6] D. Raabe, Computational Materials Science, Wiley-VCH, Weinheim, 1998.
[7] J.R. Beeler Jr., Radiation effects computer experiments, North-Holland, Amsterdam, 1983.
[8] Y. Wu, R.J. Friauf, J. Appl. Phys. 65 (1989) 4714.
[9] R. Smith (Ed.), Atomic and ion collisions in solids and at surfaces, Cambridge University Press, Cambridge, 1997.
[10] H. Haberland, Z. Insepov, M. Moseler, Phys. Rev. B 51 (1995) 11061.
[11] L.V. Zhigilei, B.J. Garrison, J. Appl. Phys. 88 (2000) 1281.
[12] S.A. Adelman, J.D. Doll, J. Chem. Phys. 64 (1976) 2375.
[13] J.C. Tully, J. Chem. Phys. 73 (1980) 1975.
[14] D.J. Diestler, M.E. Riley, J. Chem. Phys. 83 (1985) 3584.
[15] M. Moseler, J. Nordiek, H. Haberland, Phys. Rev. B 56 (1997) 15439.
[16] W. Cai, M. de Koning, V.V. Bulatov, S. Yip, Phys. Rev. Lett. 85 (2000) 3213.
[17] L.V. Zhigilei, B.J. Garrison, Mat. Res. Soc. Symp. Proc. 538 (1999) 491.
[18] L.V. Zhigilei, B.J. Garrison, SPIE Proc. Series 3254 (1998) 135.
[19] L.V. Zhigilei, B.J. Garrison, Proceedings of the International Conference on Modeling and Simulation of Microsystems, Semiconductors, Sensors, and Actuators (MSM'99), Computational Publications, Boston, 1999, p. 138.
[20] Y.B. Zel'dovich, Y.P. Raizer, Physics of Shock Waves and High-Temperature Hydrodynamic Phenomena, Vol. 2, Academic Press, New York, 1967, p. 688.
[21] Y.B. Zel'dovich, Y.P. Raizer, Physics of Shock Waves and High-Temperature Hydrodynamic Phenomena, Vol. 2, Academic Press, New York, 1967, p. 742.
[22] M.S. Daw, S.M. Foiles, M. Baskes, Mat. Sci. Rep. 9 (1993) 251.
[23] H. Gades, H.M. Urbassek, Nucl. Instrum. Meth. B 69 (1992) 232.
[24] L. Verlet, Phys. Rev. 159 (1967) 98.
[25] M.W. Finnis, J.E. Sinclair, Philos. Mag. A 50 (1984) 45.